

Metabolic analysis of osteoarthritis subchondral bone based on UPLC/Q-TOF-MS

Gang Yang¹ · Hua Zhang¹ · Tingmei Chen² · Weiwen Zhu¹ · Shijia Ding² · Kaiming Xu¹ · Zhongwei Xu¹ · Yanlei Guo³ · Jian Zhang¹

Received: 27 January 2016 / Revised: 20 March 2016 / Accepted: 24 March 2016 / Published online: 13 April 2016
© Springer-Verlag Berlin Heidelberg 2016

Abstract Osteoarthritis (OA), one of the most widespread musculoskeletal joint diseases among the aged, is characterized by the progressive loss of articular cartilage and continuous changes in subchondral bone. The exact pathogenesis of osteoarthritis is not completely clear. In this work, ultra-performance liquid chromatography coupled with quadrupole time-of-flight tandem mass spectrometry (UPLC/Q-TOF-MS) in combination with multivariate statistical analysis was applied to analyze the metabolic profiling of subchondral bone from 42 primary osteoarthritis patients. This paper described a modified two-step method for extracting the metabolites of subchondral bone from primary osteoarthritis patients. Finally, 68 metabolites were identified to be significantly changed in the sclerotic subchondral bone compared with the non-sclerotic subchondral bone. Taurine and hypotaurine metabolism and beta-alanine metabolism were probably relevant to the sclerosis of subchondral bone. Taurine, L-carnitine, and glycerophospholipids played a vital regulation role in the

pathological process of sclerotic subchondral bone. In the sclerotic process, beta-alanine and L-carnitine might be related to the increase of energy consumption. In addition, our findings suggested that the intra-cellular environment of sclerotic subchondral bone might be more acidotic and hypoxic compared with the non-sclerotic subchondral bone. In conclusion, this study provided a new insight into the pathogenesis of subchondral bone sclerosis. Our results indicated that metabolomics could serve as a promising approach for elucidating the pathogenesis of subchondral bone sclerosis in primary osteoarthritis.

Keywords Metabolomics · UPLC/Q-TOF-MS · Osteoarthritis · Subchondral bone · Metabolic pathways

Introduction

Osteoarthritis (OA) of knee joint, frequently accompanied by chronic pain and disability, is one of the most widely musculoskeletal joint diseases among the aged. The progressive loss of articular cartilage and the continuous changes in subchondral bone are two major features of OA [1]. Even though there are pathologic and radiographic evidence of osteoarthritis, most of the people have no symptoms. Epidemiological study shows that 18 % of women and 9.6 % of men of 60 or older probably have symptomatic osteoarthritis [2]. Risk factors such as sex, age, obesity, trauma, overuse, and genetics can make contributions to the process of lesions in different compartments of the joint respectively [3, 4]. The lesions of osteoarthritis involve the entire synovial joint, including the soft tissue structures, subchondral bone, and articular cartilage [5]. To date, the exact pathogenesis of osteoarthritis is not completely clear. The main characteristic of pathological changes in OA is the progressive destruction

Gang Yang and Hua Zhang contributed equally to this work.

Electronic supplementary material The online version of this article (doi:10.1007/s00216-016-9524-x) contains supplementary material, which is available to authorized users.

✉ Jian Zhang
zhangjiancqmu@sohu.com

¹ Department of Orthopedics, The First Affiliated Hospital of Chongqing Medical University, Chongqing 400016, China

² Key Laboratory of Clinical Laboratory Diagnostics (Ministry of Education), College of Laboratory Medicine, Chongqing Medical University, Chongqing 400016, China

³ Traditional Chinese Medicine Institute of Pharmaceutical Chemistry, Chongqing Institute of Traditional Chinese Medicine (TCM), Chongqing 400065, China

of articular cartilage and the sclerosis of subchondral bone [6]. In addition, soft tissue structures in and around the joint are also involved. Bridging muscles become weak. Ligaments are often lax. Synovium shows modest inflammatory infiltrates [7]. Although there are a large number of researches about the pathological changes of articular cartilage, there is surprisingly little information available on the definition and pathogenesis of subchondral bone in osteoarthritis. The subchondral bone is defined as a region which locates between the articular cartilage and the marrow cavity [8]. In the joint, the articular cartilage and subchondral bone act as a functional unit [9]. It has been considered all the time that the early pathological changes of articular cartilage can result in the changes of subchondral bone and then induce a series of pathological changes of the osteoarthritis, so most of fundamental researches on the pathogenesis of osteoarthritis are focused on the articular cartilage. However, inhibiting the activity of TGF- β 1 in subchondral bone made the pathological changes of osteoarthritis attenuated and led to less degeneration of articular cartilage compared with control groups in the osteoarthritis rodent models [10]. It suggested that the pathological changes of subchondral bone may play an important role in the initiation and development of osteoarthritis.

Metabolomics, a branch of the systems biology, studies the metabolite compositions of biological fluid, cell, and tissue in a biological system. The analysis of the complete set of metabolites has been applied to biological research for more than a decade [11]. Metabolomics has generated great interest for disease diagnosis, pathological mechanism research, drug toxicology research, drug safety evaluation, and so on [12–15]. Metabolomics studies the end-products of bioprocesses. These end-products cover a diverse group of low molecular weight ($M < 1000$) organic and inorganic compounds that represent the functional status in a biology system under a given condition [16]. The most frequently used analytical technologies in metabolomics are nuclear magnetic resonance spectroscopy (NMR), gas chromatography–mass spectrometry (GC-MS), and liquid chromatography–mass spectrometry (LC-MS) [17]. Each technique has its advantages and disadvantages. Compared with the conventional LC methods, the ultra-performance liquid chromatography (UPLC) achieves an even higher sensitivities, higher resolutions, and rapid separations [18, 19]. Therefore, ultra-performance liquid chromatography–mass spectrometry (UPLC-MS) attracts more and more interest in metabolomics research.

Metabolic perturbations in urine, blood, synovial fluid (SF), and synovium from patients and animal models with osteoarthritis have been detected using metabolic analytical technologies [20]. Urine from patients with osteoarthritis was studied using GC-MS. The up-regulated TCA cycle was identified to be associated with osteoarthritis. Knee joint effusion symptom was accompanied with the histamine metabolism disorder [21]. Serum from patients with osteoarthritis was

analyzed based on NMR. The researchers demonstrated that the ratios of leucine and valine to histidine were predictive of osteoarthritis [22]. SF from experimentally induced osteoarthritis in canine knee joints was performed metabolomics analysis via NMR. The investigators concluded that the intra-articular environment of osteoarthritis was more hypoxic and acidotic than the normal joint [23]. The conditioned media collected from the explant cultures of osteoarthritis patients synovium was studied using GC-MS and LC-MS. Eleven metabolites were obviously increased in the end-stage osteoarthritis patients [24]. Knee joint SF of patients with osteoarthritis was also studied using NMR and GC-MS. Eleven metabolites were statistically important for the separation between SF of osteoarthritis and normal SF [25]. Current researches have shown some evidence of metabolic alterations associated with osteoarthritis. However, no research has been done to explore the metabolic perturbations in subchondral bone from osteoarthritis patients using the metabolomics technology. By the metabolic analysis of subchondral bone, we could find more metabolic alterations associated with osteoarthritis, thereby elucidating the molecular mechanism of the subchondral bone sclerosis in osteoarthritis.

In this study, sclerotic subchondral bone and non-sclerotic subchondral bone were collected from 42 patients with osteoarthritis of knee joint. Non-targeted metabolomic analysis was performed using ultra-performance liquid chromatography coupled with quadrupole time-of-flight tandem mass spectrometry (UPLC/Q-TOF-MS). Multivariate statistical analysis was applied to identify the varied metabolites which were response for the discrimination between the experiment group and control group. The non-targeted investigation of metabolites was utilized to analyze the metabolic profiling of subchondral bone in osteoarthritis and determine the most relevant metabolic pathways to the sclerosis of subchondral bone, with the aim to explore the molecular mechanism of the sclerosis of subchondral bone in osteoarthritis.

Materials and methods

Chemical and materials

The reference standards for taurine, L-tyrosine, hypoxanthine, L-carnitine, uridine, guanosine, 2-hydroxycinnamic acid, triethanolamine, 2-phenylacetamide, octadecylamine, and retinol acetate were purchased from MCGBW (Beijing, China). HPLC-grade acetonitrile and formic acid were purchased from Sigma-Aldrich (St. Louis, MO, USA). Methanol and dichloromethane were obtained from Tedia (Fairfield, OH, USA). Distilled water was acquired by a Milli-Q Ultra-pure water system (Millipore, Billerica, USA). Scalpel and rongeur (LZQ, Shanghai, China). Pressure Blowing Concentrator MTN-2800D from AUTO&SCIENCE, Tianjing, China.

High-throughput tissue grinder SCIENTZ-48 from SCIENTZ, Zhejiang, China. UPLC/Q-TOF-MS was purchased from AB Sciex™, USA and GC-MS from Agilent 7890A, USA.

Experimental participants

All of the 42 experimental participants were recruited from inpatients of The First Affiliated Hospital of Chongqing Medical University. The diagnosis of knee joint osteoarthritis was performed according to the American College of Rheumatology (ACR) criteria for osteoarthritis [26]. The inclusive criteria of experimental participants were that all primary osteoarthritis patients displayed radiological information (weight-bearing antero-posterior and lateral views) of knee joint on radiograph with a radiological grade 3 on the Kellgren-Lawrence (KL) scale [27]. The exclusive criteria of experimental participants were that patients with history of drug use and patients with osteoarthritis led by trauma or other reasons. Based on the above procedures, a total of 60 patients with knee joint osteoarthritis were recruited, but 18 of them with history of knee surgery, trauma, or drug use were excluded. At last, 42 patients with primary osteoarthritis of knee joint were qualified for this study. The centric subarticular spongiosa of the medial femoral condyle was sampled as the experimental group, and the centric subarticular spongiosa of the lateral medial femoral condyle was sampled as the control group.

Sample collection and preparation

The samples were immediately collected after patients undergoing total knee replacement and then temporarily stored in a 5-L liquid nitrogen container. All the samples were transferred to a 50-L liquid nitrogen container and stored at -80°C until analysis.

To minimize the potential changes of component in sample before solvent extraction, all samples were thawed on ice for 20 min. Cartilage was carefully removed from the femoral condyle by excision with a scalpel. Centric subarticular spongiosa was sampled from the femoral condyle using a rongeur. The subarticular spongiosa was crumbed by rongeur and then grounded into powder in liquid nitrogen. A weighed amount of subchondral bone (100 mg) was subaliquotted into a 2-mL vial. Before the extraction of metabolites, a modified two-step method to extract the metabolites of subchondral bone was preliminary tested by GC-MS and UPLC/Q-TOF-MS [28]. Results revealed that the modified two-step method was performed successfully to cover the aqueous and organic metabolites. Thus, the modified two-step extraction method could be used for extracting the metabolites of subchondral bone. Firstly, 1 mL methanol–water (3:1, *v/v*) was added for protein precipitation and tissue homogenate using a 47-bead-

based high-throughput tissue grinder (twice, 40 Hz, 5 min). The mixture was vortex-mixed violently for 20 s and subsequently centrifuged at 12,000 rpm for 10 min, and then 600 μL supernatant was transferred into a 1.5-mL vial. Secondly, 1 mL dichloromethane–methanol (1:3, *v/v*) was added for performing subsequent extraction. The mixture was vortex-mixed for 20 s and centrifuged at 12,000 rpm for 10 min, and then 600 μL supernatant was transferred into the 1.5-mL vial again. At last, the mixed supernatant was centrifuged at 12,000 rpm for 10 min, and 1 mL mixed supernatant was transferred into a new 1.5 mL vial. The mixed supernatant was evaporated to dryness at 45°C with nitrogen in a pressure blowing concentrator. Dry residue redissolved in 100 μL acetonitrile–water (50:50, *v/v*) and centrifuged at 12,000 rpm for 10 min. Sixty microliters of resulting supernatant was transferred into the autosampler vial. Ten microliters of resulting supernatant of each sample was transferred into the QC vial.

Validation of analytical method

The quality control sample (QC), the mixture of equal amounts of each sample, was prepared to monitor the stability and repeatability of the analytical system [29]. At the start of the analysis of each sample batch, ten QC samples were run to ensure that the system had reached equilibrium [28]. Then, one QC sample was run at regular intervals (six samples) throughout the analytical process to assess the stability and repeatability of the system. One blank sample (the distilled water) was then analyzed after each of the interval QC sample in order for background correction and to monitor the lack of cross-contamination [30]. The QC data sets were performed by principal component analysis (PCA) to assess the stability and repeatability of the system. Furthermore, the reproducibility of the ions was evaluated by relative standard deviation (RSD%) of randomly picked peaks from the 13 within-run QC samples in RPLC_Neg, RPLC_Pos, HILIC_Neg, and HILIC_Pos ion modes respectively.

UPLC/Q-TOF-MS analysis

UPLC/Q-TOF-MS (AB Sciex™, USA) analysis was conducted using a Shimadzu UPLC-equipped AB-Sciex Triple TOF 4600 and operated in both positive and negative ionization mode using the Turbo V ESI ion source. The samples were injected into an Kinetex XB-C18 column (100 mm \times 2.1 mm, 2.6 μm , Phenomenex) with a flow rate of 0.35 mL/min. Gradient elution was performed using a mixture solvent A (0.1 % formic acid in water) and solvent B (100 % acetonitrile). The gradient used was as follows: solvent B (acetonitrile) was held at 5 % for 1 min and solvent B was increased from 5 to 85 % over 5 min, following solvent B was held at 85 % by 8 min and then was shifted to 5 % by 8.1 min. At last, solvent B was held constantly at 5 % to

10 min. The ion spray voltage was set to 5500 V for positive ion and -4500 V for negative ion mode respectively. The nebulizer gas (air) and turbo gas (air) were both set to 55 psi, and the heater temperature was 600 °C. The curtain gas (nitrogen) was set at 25 psi, the rolling collision energy was set to 40 ± 15 (ESI+) or -40 ± 15 V (ESI-), and the collision cell pressure was set at low or high mode for different purposes. Full scan analysis was performed in the EMS mode using the electrospray ionization technique with a coverage of mass range of 50 to 1000 Da, with a data acquisition rate set to 0.25 s for TOF-MS scan and 0.1 s for MS/MS scan. Eight data were obtained in one acquisition, and the MS/MS scan was accomplished in the combinational mode of positive information-dependent acquisition (IDA). Ten microliters of sample was injected to be analyzed. The run order of samples was random. All samples were stored at 4 °C during the analysis.

Data analysis

Data processing

After the UPLC/Q-TOF-MS analysis, the raw data from all the samples were processed using MarkerView v1.2.1 software (AB SCIEXTM, USA). Pre-treatment procedures of baseline correction, denoising, deconvolution, alignment, and normalization were performed to process the raw data. The relevant parameters used were retention time (RT) range 0.1–10 min, minimum spectral peak width 25 ppm, minimum RT peak width 6 scan, mass tolerance 0.01 kDa, RT tolerance 0.1 min, noise threshold 100, maximum number of peaks 2000, excluding isotopic peaks. The resulting three-dimensional matrix was composed of sample names, *m/z* and RT pairs, and normalized ion intensities. The “80 % rule” was applied to remove missing peaks [31], and then the remaining missing values were imputed using regularized expectation maximization. The data was then pareto scaled and mean centered before multivariate data analysis.

Multivariate data analysis and statistics

The final data set was imported into the SIMCA-P 13.0 software (Umetrics AB, Umeå, Sweden) to perform the unsupervised principal component analysis (PCA) and supervised orthogonal partial least squares-discriminant analysis (OPLS-DA) [32]. The varied metabolites responsible for the discrimination were identified between the experiment group and control group. Non-parametric test was applied to evaluate the significant differences in the variables using the SPSS 17.0 software (IBM, USA). The *p* values <0.05 were considered to be statistically significant.

Metabolite identification and metabolic pathway analysis

According to *m/z* and RT pairs, the metabolites were preliminarily identified via online HMDB (<http://www.hmdb.ca/>) database with mass tolerance of less than 0.01 Da. The potential metabolites can be further identified by the comparison of MS or MS/MS spectra integrated in PeakView v1.2 software (Umetrics AB, Umeå, Sweden), with available reference standard mass spectral databases, such as HMDB and Mass Bank (<http://www.massbank.jp/>), and then part of the potential metabolites was confirmed by analyzing the authentic chemical standard substances. In order to explore the molecular mechanism of the sclerosis of subchondral bone, the KEGG (<http://www.kegg.com/>) and PubMed (<http://www.ncbi.nlm.nih.gov/>) database were utilized to search the metabolic pathway and biological function of the metabolites. Ultimately, the metabolic pathway analysis was performed using MetPA (<http://metpa.metabolomics.ca/MetPA/faces/Home>) [33] via database source including the HMDB, KEGG, SMPD (<http://www.smpdb.ca/>) and METLIN (<http://metlin.scripps.edu/>) for confirming the impacted metabolic pathways and visualization. Figure 1 displayed a roadmap for sample collection through to data analysis and metabolites identification.

Results

Demographics and clinical characteristics

The demographics and clinical characteristics of experiment group and control group were depicted in Table 1. Because the samples of experiment group and control group were derived from the same patient, there was no difference in age, height, weight, and BMI between two groups. A common feature of these participants was that the medial knee joint space became extremely narrow, and the lateral knee joint space was relatively normal. There was no articular cartilage covering the surface of the subchondral bone in the medial femoral condyle. Besides, the subchondral bone of the medial femoral condyle had changed in physicochemical property compared with the subchondral bone of the lateral medial femoral condyle.

Medicine image of subjects and histological analysis of the samples

The results of the typical X-ray image and the picture of specimen were matched with the subchondral bone biopsy report (gold standard). Figure 2 displayed the comparison of the sclerotic subchondral bone and non-sclerotic subchondral bone in imageology, specimen, and pathology. In imageology and specimen, letters “E” and “C” refer to the sample position. The sclerotic subchondral bone and non-sclerotic subchondral

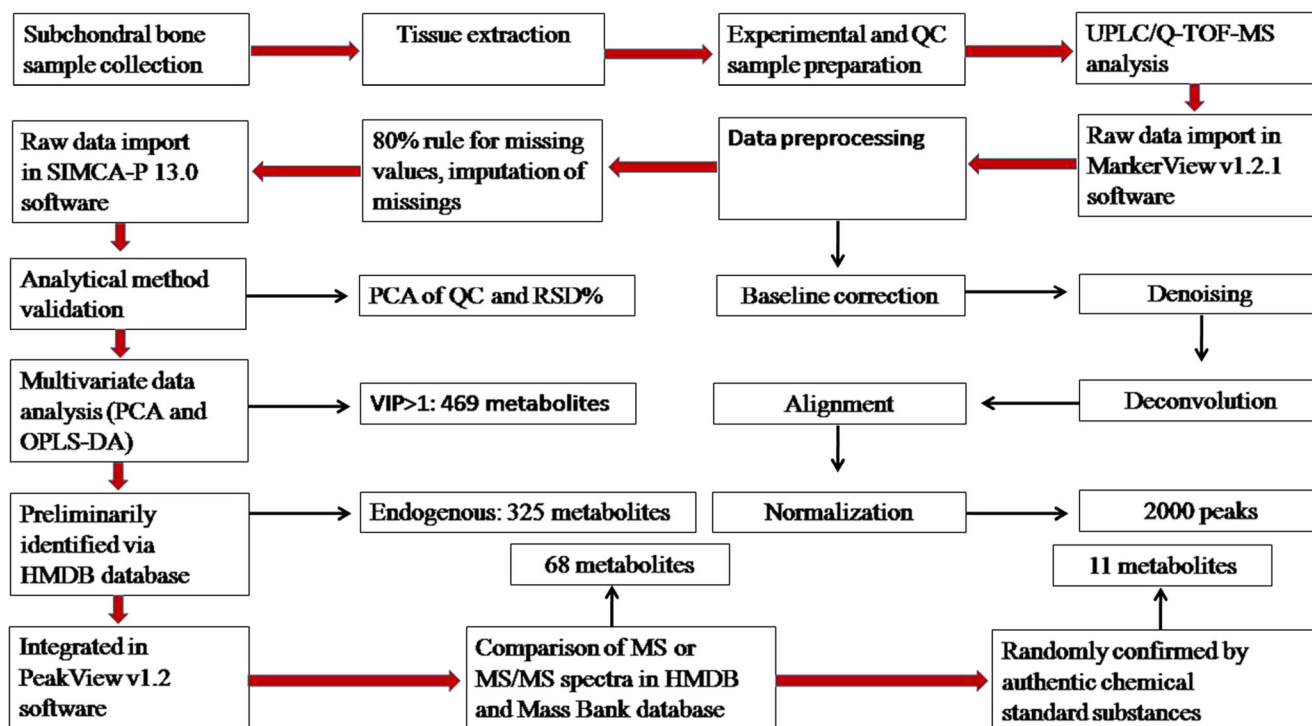


Fig. 1 UPLC/Q-TOF-MS based roadmap for the metabolic profiling of subchondral bone showing the steps involved in preparing and analyzing both the QC sample and study samples

bone were identified by pathological section. The formation of new extra bone on trabeculae and microfracture, two typical features of sclerotic subchondral bone, were presented in the subchondral bone of experiment group. The pathologic picture of control group displayed a normal structure of subchondral bone. It revealed that the experiment group was sclerotic subchondral bone, and the control group was non-sclerotic subchondral bone.

Analytical method validation

In UPLC/Q-TOF-MS-based metabolomics, analytical performance can gradually change over time because of the changes of temperature and sample pH, contamination, and a decline

Table 1 Demographic description and clinical characteristics of participants in the study

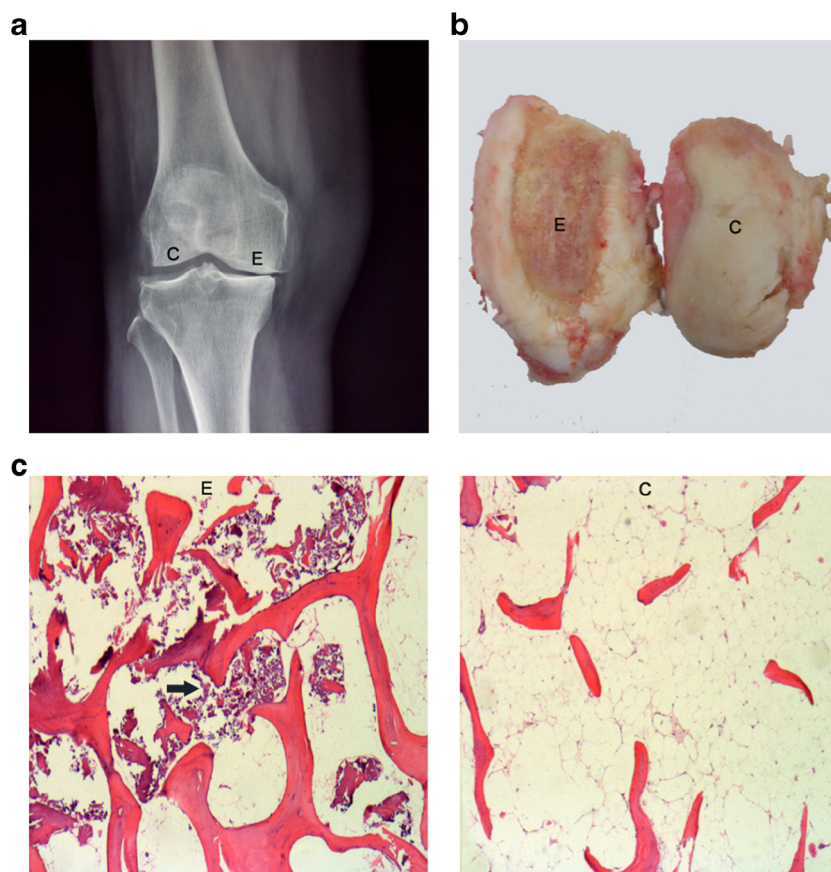
	Experiment group	Control group
Age (years)	66.2 ± 6.8	66.2 ± 6.8
Total number	42	42
Female number	37	37
Sclerosis of subchondral bone	Yes	None
Joint space narrow grade	Severely	Mild or none
Cartilage coverage	None	Yes
History of knee trauma	None	None
History of drug use	None	None

in the responses of the MS [28]. Assessing the repeatability and stability of the analytical system is an extremely important component of metabolomic profiling studies. Ninety-two QC samples were used to perform the unsupervised principle component analysis (PCA). A PCA model with R2Xcum of 0.613 and Q2cum of 0.547 was achieved (see Electronic Supplementary Material (ESM) Fig. S1). In PCA analysis, the repeated QC samples were separately clustered in four small spaces in scores plots in accordance with the four detection ion modes. Because the close degree of QC samples cluster on the score plot was positive correlation with the stable of the analysis [34], this result indicated that the reproducibility was favorable. Furthermore, the reproducibility of the ions was evaluated by relative standard deviation (RSD%) of 8 randomly picked peaks in the 13 within-run QC samples. The results (see ESM Table S1) indicated that the UPLC/Q-TOF-MS system had good stability and reproducibility.

Multivariate analyses of the metabolic profiles

As the principal component analysis (PCA) was the most commonly used unsupervised method in metabolomics studies, PCA was carried out in this study to obtain an initial overview of the data set. In PCA analysis, the two groups were mainly separated in the UPLC/Q-TOF-MS positive and negative ion mode (see ESM Fig. S2). For supervised multivariate statistical analysis, orthogonal partial least squares-discriminant analysis (OPLS-DA) was carried out to identify

Fig. 2 Comparison of the experiment group (*E*) and control group (*C*) in imageology (**a**), specimen (**b**), and pathology (**c**). Letters *E* and *C* in imageology and specimen refer to the sample position. In pathological section (4 \times), the formation of new extra bone on trabeculae and microfractures (*black arrow*) was found in the subchondral bone of experimental group and could not be found in the subchondral bone of control group. It revealed that the experiment group was sclerotic subchondral bone and the control group was non-sclerotic subchondral bone



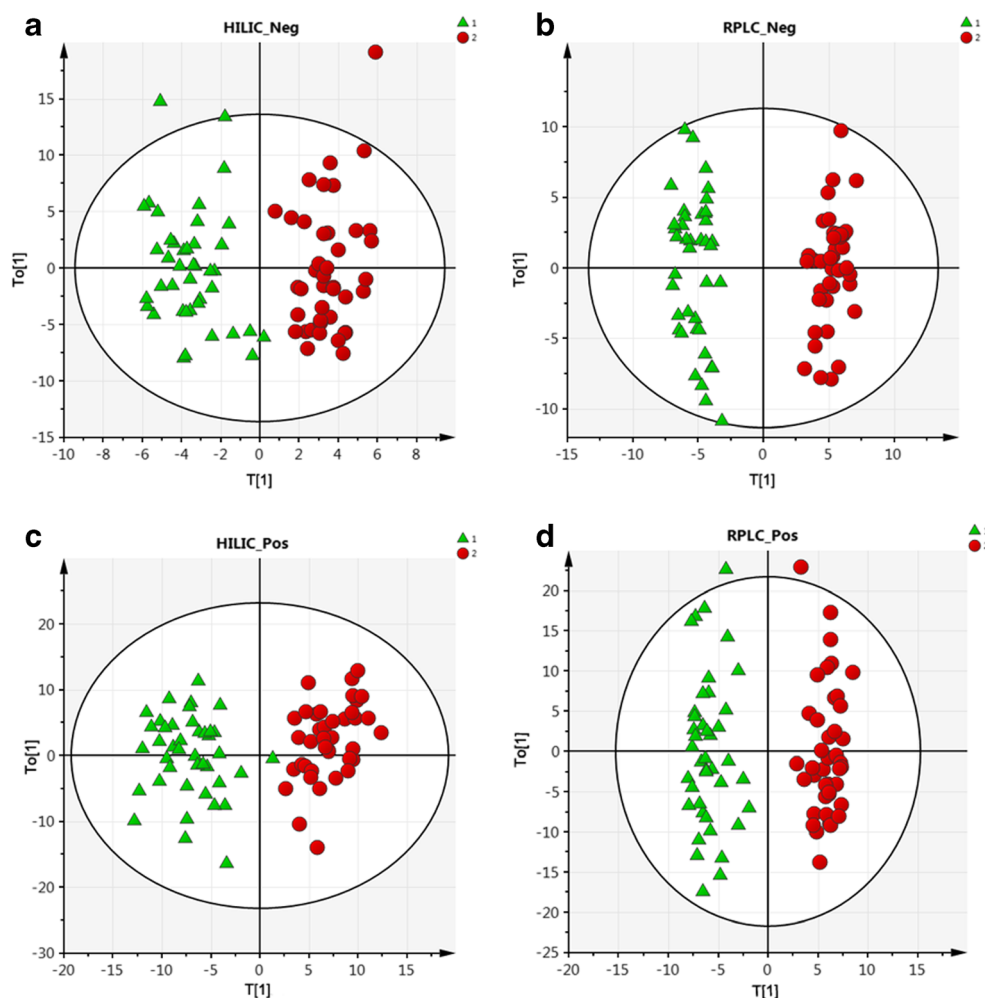
the varied metabolites responsible for discrimination in this study. In UPLC/Q-TOF-MS hydrophilic interaction liquid chromatography-negative (HILIC_Neg) ion mode analysis, an OPLS-DA model with R^2Y_{cum} of 0.866 and Q^2_{cum} of 0.751 was achieved (Fig. 3a). In UPLC/Q-TOF-MS reversed phase liquid chromatography-negative (RPLC_Neg) ion mode analysis, an OPLS-DA model with R^2Y_{cum} of 0.964 and Q^2_{cum} of 0.913 was achieved (Fig. 3b). In UPLC/Q-TOF-MS hydrophilic interaction liquid chromatography-positive (HILIC_Pos) ion mode analysis, an OPLS-DA model with R^2Y_{cum} of 0.92 and Q^2_{cum} of 0.65 was achieved (Fig. 3c). In UPLC/Q-TOF-MS reversed phase liquid chromatography-positive (RPLC_Pos) ion mode analysis, an OPLS-DA model with R^2Y_{cum} of 0.912 and Q^2_{cum} of 0.806 was achieved (Fig. 3d). The quality of OPLS-DA model was evaluated by the R^2 and Q^2 values. R^2 represents the goodness-of-fit parameter of the OPLS-DA model. Q^2 represents the predictability parameter of the OPLS-DA model. R^2 and Q^2 values greater than 0.5 indicate high quality of OPLS-DA models [35]. In our study, all the models displayed greater than 86.6 % of the goodness-of-fit ($R^2Y=0.866-0.964$) and a predictability greater than 65 % ($Q^2=0.65-0.913$), which indicated that these OPLS-DA models were performed successfully to represent the differences of the metabolites in two groups.

Because the potential metabolites with variable importance in the projection (VIP) greater than 1 were responsible for the apparent discrimination in OPLS-DA models, 154 metabolites out of 536 variables in RPLC-positive ionization mode, 88 metabolites out of 235 variables in RPLC negative ionization mode, 175 metabolites out of 473 variables in HILIC-positive ionization mode, and 52 metabolites out of 146 variables in HILIC-negative ionization mode were picked out. In total, 469 metabolites were picked out for further identification.

Identification of potential metabolites

The metabolites with $VIP > 1$ were preliminarily identified via online HMDB database with mass tolerance of less than 0.01 kDa. The potential metabolites were further identified by the comparison of MS or MS/MS spectra with available reference standard mass spectral databases and then confirmed by analyzing the authentic chemical standard substances. According to these procedures, 68 out of 469 metabolites in our study were identified (see ESM Table S2). The content of trichocarposide, LysoPC (P-16:0), LysoPC (P-18:1 (9Z)), N6,N6,N6-trimethyl-L-lysine, 5-(4'-hydroxyphenyl)-gamma-valerolactone-4'-O-glucuronide, SM (d18:1/22:1 (13Z)), and SM (d16:1/24:1

Fig. 3 OPLS-DA score plots of four modes based on subchondral bone metabolic profiling of the experiment group (*triangles*) and control group (*circles*)



(15Z)) were found to be decreased in the sclerotic subchondral bone. Others were found to be increased in the sclerotic subchondral bone. Identification of taurine (HMDB00251), L-tyrosine (HMDB00158), hypoxanthine (HMDB00157), L-carnitine (HMDB00062), uridine (HMDB00296), guanosine (HMDB00133), 2-hydroxycinnamic acid (HMDB02641), triethanolamine (HMDB32538), 2-phenylacetamide (HMDB10715), octadecylamine (HMDB29586), and retinol acetate (HMDB35185) were confirmed by analysis of standard solutions under the same instrumental conditions. The correlation between the relative abundance of validated metabolites and the samples was examined using correlation coefficients (Fig. 4). All the 68 metabolites with P values less than 0.05 were significant evaluated by non-parametric test.

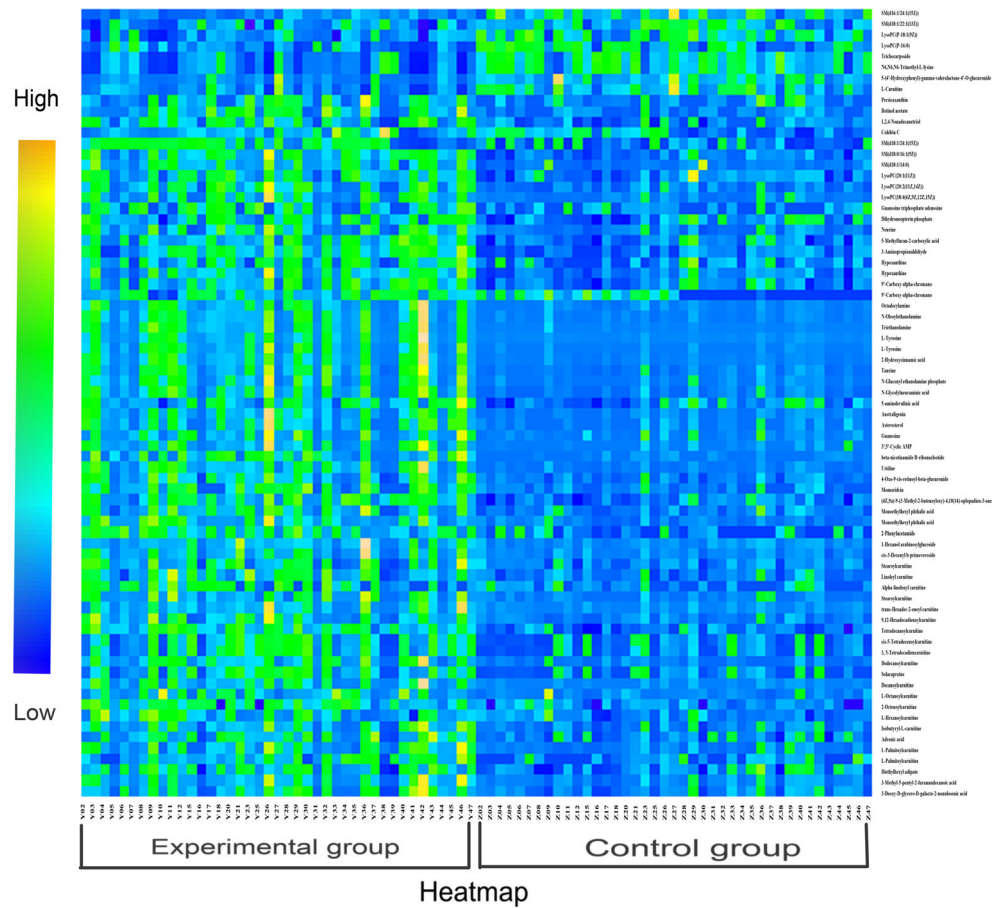
Relevant metabolic pathways

In order to explore the relationship between the 68 selected metabolites and the sclerosis of subchondral bone in

osteoarthritis, the metabolic pathway analysis (MetPA) was performed to identify the most relevant pathways of the identified metabolites. The relevant metabolic pathways were presented on a panel, in which all the matched pathways were displayed as circles. The size and color of each circle are based on pathway impact value and p value, respectively. Global test was performed for pathway enrichment analysis. Relative-betweenness centrality was performed for pathway topology analysis. The circles on the top right diagonal region of panel indicated that the metabolites involved in those pathways were significantly changed. Due to their important positions, these alterations were more likely to have big impacts on those pathways. In a general way, the pathway impact value of greater than or equal to 0.01 indicated that the pathway was significantly changed.

Metabolic pathway analysis revealed that taurine and hypotaurine metabolism, beta-alanine metabolism, phenylalanine metabolism, tyrosine metabolism, lysine degradation, pyrimidine metabolism, purine metabolism, and sphingolipid metabolism were related to the sclerosis of subchondral bone in osteoarthritis (Fig. 5). In which, taurine and hypotaurine

Fig. 4 The correlation heatmap between the level of metabolites and the samples



metabolism with an impact factor of 0.33 and beta-alanine metabolism with an impact factor of 0.10 were found to be the most relevant pathways to osteoarthritis. Metabolic pathway analysis revealed that taurine belonged to taurine and

hypotaurine metabolism and 3-aminopropionaldehyde belonged to beta-alanine metabolism. The metabolites that supported the metabolic pathway analysis were shown as the box plots (see ESM Fig. S3).

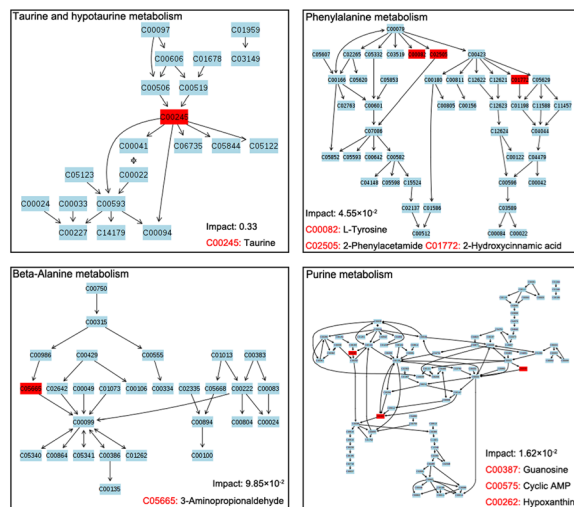
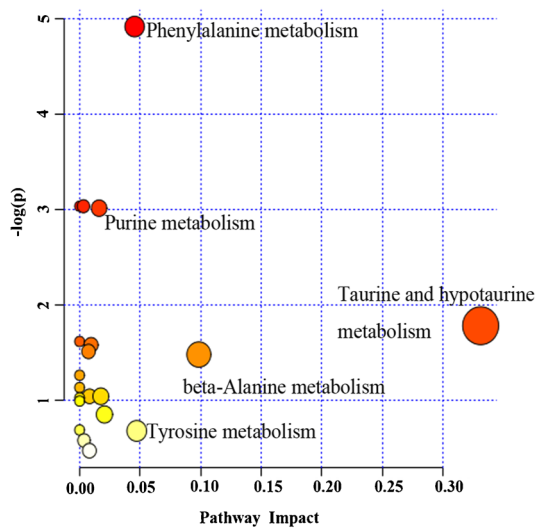


Fig. 5 Metabolic pathway analysis of the identified metabolites in osteoarthritis. The metabolomics pathways were arranged according to the scores based on topology (*x-axis*) and enrichment analysis (*y-axis*)

Discussion

The metabolic analysis platforms have been applied to study osteoarthritis for many years. Metabolic disturbances in synovium, synovial fluid (SF), blood, and urine of osteoarthritis patients and animal models have been analyzed using NMR, GC-MS, and LC-MS [20]. Great achievements have been acquired in these researches. However, the subchondral bone does not catch the researcher's close attention due to the difficulty of obtaining the subchondral bone sample and processing bone tissue. The lesions of subchondral bone are accompanied with articular cartilage destruction in osteoarthritis. The formation of new extra bone on trabeculae and microfractures can occur in subchondral bone during the progression of osteoarthritis [36]. New bone synthesis exceeds degradation in patients with knee joint osteoarthritis [37]. Thus, the bone mineral density of subchondral bone with lesions is higher than the normal, leading to the sclerosis of subchondral bone eventually. However, the exact molecular mechanism of subchondral bone sclerosis in osteoarthritis is not completely clear. Recent studies have revealed that abnormal subchondral bone cell metabolism plays a potential role in the initiation and progression of osteoarthritis. This implies that powerful tools need to be applied to explore the alteration of sclerotic subchondral bone cell metabolism in osteoarthritis.

In this study, an UPLC/Q-TOF-MS-based metabolomics analysis was performed to explore the abnormal cellular metabolism in subchondral bone using a modified two-step extraction method. By applying the multivariate statistical analysis, 68 metabolites that significantly contributed to this discrimination were identified, including the fatty acyls, benzene and substituted derivatives, prenol lipids, nucleotides, steroids and steroid derivatives, carboxylic acids and derivatives, glycerophospholipids, sphingolipids, amines, phenylpropanoic acids, and so on. Hypoxanthine was detected to be enriched in urine from guinea pigs with OA using nuclear magnetic resonance [38]. Tyrosine was detected to be enriched in blood from sheep with OA using nuclear magnetic resonance [39]. Uridine and tyrosine were detected to be enriched in synovial fluid from ovine with early OA using nuclear magnetic resonance [40]. In the present study, an increase of hypoxanthine, tyrosine, and uridine were also found in sclerotic subchondral bone from osteoarthritis patients. In addition, L-palmitoylcarnitine, monoethylhexyl phthalic acid, L-tyrosine, hypoxanthine, and 9'-carboxy-alpha-chromanol were found to be increased in sclerotic subchondral bone compared with the control in both positive and negative ionization modes.

In this work, decanoylcarnitine, alpha-linolenyl carnitine, trans-hexadec-2-enoyl carnitine, L-palmitoylcarnitine, 9,12-hexadecadienoylcarnitine, and dodecanoylcarnitine were found to be up-regulated in the sclerotic subchondral bone, all of which belonged to the acylcarnitine. Okun's study revealed that acylcarnitine was useful in the diagnosis of fatty

acid oxidation disorders [41]. Therefore, the up-regulation of these metabolites in sclerotic subchondral bone suggested that the intra-cellular environment of sclerotic subchondral bone might be more hypoxic and acidotic compared with the non-sclerotic subchondral bone. *Damyanovich* concluded that the intra-articular environment of osteoarthritis was more hypoxic and acidotic compared to the normal joint [23]. Thus, we could speculate that the abnormal intra-articular environment of osteoarthritis might be partially caused by the sclerosis of subchondral bone.

Glycerophospholipids and sphingolipids occupied a large part of the distinctive metabolites between two groups, such as LysoPC (P-16:0), LysoPC (P-18:1 (9Z)), LysoPC (18:4 (6Z, 9Z,12Z,15Z)), LysoPC (20:2 (11Z,14Z)), LysoPC (20:1 (11Z)), SM (d18:0/16:1 (9Z)), SM (d18:1/22:1 (13Z)), SM (d16:1/24:1 (15Z)), SM (d18:1/24:1 (15Z)), SM (d18:1/14:0). Most of them were up-regulated in sclerotic subchondral bone. Glycosphingolipids were ubiquitous cell membrane components and play important roles in the development and function of several tissues. It can modulate transmembrane signalling and mediate cell-to-cell and cell-to-matrix interactions [42]. Glycosphingolipids were necessary for the RANKL-induced osteoclastogenesis [43]. The inhibition of glycosphingolipid synthesis limited the osteoclast activation [44]. It indicated that the catabolism of sclerotic subchondral bone was enhanced. These discoveries agreed with *Mansell's* results of high bone turnover rate in the sclerotic subchondral bone [45]. Glycerophospholipids and sphingolipids were detected to be enriched in synovial fluid from patients with early and late stages of OA using LC-MS/MS. Moreover, sphingolipids can alter synovial inflammation and the repair responses of damaged joints [46]. In brief, glycerophospholipids and sphingolipids play a vital regulation role in the pathological process of sclerotic subchondral bone.

L-Carnitine, involved in the transport of acetyl-CoA into mitochondria, was the critical point of carnitine-dependent transport of long-chain fatty acids and indispensable for β -oxidation [47, 48]. Specification and differentiation of osteoblasts in bone and global energy homeostasis was regulated by inducing the expression of key enzymes required for fatty acid β -oxidation [49]. L-Carnitine significantly enhanced the proliferation and differentiation of human osteoblast in vitro. Also, L-Carnitine significantly increased osteoblast activity [50]. By the IGF-1/PI3K/Akt signalling pathway, L-carnitine showed an important role in osteoblast differentiation and mineralization of NIH3T3 fibroblasts. 10 μ M L-carnitine positively affected the proliferation of NIH3T3 cells, but 100 μ M L-carnitine slightly inhibited cell proliferation [51]. According to the study of *Orsal E*, carnitine presented a protective bone-sparing effect on osteoporosis induced by ovariectomy and inflammation in rats [52]. L-Carnitine protected against apoptosis of rat bone marrow cell and murine MC3T3-E1 osteoblastic cells [53, 54]. In addition, L-carnitine expedited the

recovery of normal BV/TV level after a hypocalcemic diet [55]. Under osteoporotic and/or inflammatory conditions, carnitine could enhance the healing of bone fracture [56]. Taken together, L-carnitine acted an important role in energy metabolism and bone formation, provided a new reasonable explanation on the sclerosis of subchondral bone in osteoarthritis.

Metabolic pathway analysis revealed that taurine and hypotaurine metabolism with an impact factor of 0.33 was clearly found to be relevant to the sclerosis of subchondral bone in osteoarthritis. Taurine was belonged to the taurine and hypotaurine metabolism. Our results showed that the level of taurine in sclerotic subchondral bone was up-regulated. Taurine was existed in many kinds of tissues and relevant to many crucial physiological functions [57]. Taurine was enriched in the bone cells [58]. In addition, taurine was identified to be beneficial in the promotion of bone tissue formation, as evidenced by promoting human mesenchymal stem cells to differentiate into osteoblast [59] and promoting collagen synthesis and matrix formation [60–62]. Besides promoting bone tissue formation, taurine also restrained bone tissue degradation through inhibiting the osteoclast formation and bone resorption [63]. Interestingly, taurine supplementation had been shown to increase bone mineral density in rats [64]. Taken together, these studies revealed that taurine could promote bone tissue formation and inhibit bone tissue degradation at the molecular and cellular level. Besides, Hügle found that taurine was existed in synovial fluid in osteoarthritis [65]. Thus, it could put the hypothesis that the disturbance of taurine and hypotaurine metabolism in subchondral bone has a direct correlation with the sclerosis of subchondral bone in osteoarthritis. It could provide a new reasonable explanation on the sclerosis of subchondral bone in osteoarthritis because the sclerosis of subchondral bone is the early clinical manifestation of osteoarthritis. Thus, taurine could be used as an early biomarker for the sclerosis of subchondral bone in osteoarthritis if this change could be detected in urine or blood. Therefore, further studies are required to confirm this hypothesis in urine or blood of osteoarthritis.

Many studies supported the result that beta-alanine was increased in urine, synovium, and synovial fluid from the animal models with osteoarthritis [39, 41, 65]. In this study, metabolic pathway analysis revealed that beta-alanine metabolism was found to be relevant to the sclerosis of subchondral bone in osteoarthritis, with an impact factor of 0.10. 3-Aminopropionaldehyde belonged to the beta-alanine metabolism. The level of 3-aminopropionaldehyde was found to be up-regulated in sclerotic subchondral bone. In the beta-alanine metabolism pathway, 3-aminopropionaldehyde could be metabolized into beta-alanine. Therefore, it had the possibility that beta-alanine might also be increased in the sclerotic subchondral bone though we did not detect this change. Numerous studies revealed that beta-alanine could enhance working capacity and power output in the muscle cell [66]. However, there was no

report about the function of beta-alanine in the bone cell. Because the osteoblast and osteoclast activity were increased in sclerotic subchondral bone, energy consumption was increased in bone cell. Therefore, we could infer that beta-alanine might have the similar role in both muscle cell and bone cell. Thus, further studies should be performed to explore the disturbance of beta-alanine metabolism in bone cell of the sclerotic subchondral bone from osteoarthritis patients.

Our future work will dedicate to investigate the relationship between the concentration of potential metabolites and the sclerosis degree of subchondral bone in osteoarthritis. In addition, these potential metabolites will be analyzed in serum and urine of patients with osteoarthritis, with the aim to identify the potential biomarkers for the sclerosis of subchondral bone in osteoarthritis.

Conclusions

Our results highlight the power of UPLC/Q-TOF-MS-based metabolomics approach in combination with multivariate statistical analysis for studying the metabolic profile in sclerotic subchondral bone from osteoarthritis patients. In this work, a modified two-step extraction method was successfully performed to extract the metabolites of bone tissue. In addition, 68 metabolites were found to be distinctly different between the sclerotic subchondral bone and non-sclerotic subchondral bone. Most of them were increased in the sclerotic subchondral bone. Our results suggested that the intra-cellular environment of sclerotic subchondral bone might be more hypoxic and acidotic compared with the non-sclerotic subchondral bone. Alteration in taurine and beta-alanine metabolism was clearly found to be associated with the sclerosis of subchondral bone. Taurine, L-carnitine, and glycerophospholipids played a vital regulation role in the pathological process of sclerotic subchondral bone. In the sclerotic process of subchondral bone, beta-alanine and L-carnitine might be related to the increase of energy consumption. These findings provided a new reasonable explanation on the sclerosis of subchondral bone in primary osteoarthritis. Therefore, further studies are required to confirm these inferences.

Acknowledgments This study was funded by National Natural Science Foundation of China (no. 89011060). The authors sincerely thank the subjects who participated in the study. The authors are also acknowledged for the sample collection at The First Affiliated Hospital of Chongqing Medical University, Chongqing, China.

Compliance with Ethical Standards

Conflict of interest All the authors declare that they have no conflict of interest. The experiment designed for this study involved subchondral bone from 42 patients with primary osteoarthritis. The experiment was approved by the ethics committee of Chongqing Medical University. Written informed consent was obtained from each individual participant.

References

- Hinman RS, Crossley KM. Patellofemoral joint osteoarthritis: an important subgroup of knee osteoarthritis. *Rheumatology (Oxford)*. 2007;46(7):1057–62.
- Pereira D, Ramos E, Branco J. Osteoarthritis. *Acta Med Port*. 2015;28(1):99–106.
- Abramson SB, Attur M. Developments in the scientific understanding of osteoarthritis. *Arthritis Res Ther*. 2009;11(3):227.
- Luo SX, Li S, Zhang XH, et al. Genetic polymorphisms of interleukin-16 and risk of knee osteoarthritis. *PLoS One*. 2015;10(5), e0123442.
- Swift A. Osteoarthritis 1: physiology, risk factors and causes of pain. *Nurs Times*. 2012;108(7):12–5.
- Loeser RF. Osteoarthritis year 2013 in review: biology. *Osteoarthritis Cartilage*. 2013;21(10):1436–42.
- Scanzello CR, Loeser CR. Inflammatory activity in symptomatic knee osteoarthritis: not all inflammation is local. *Arthritis Rheumatol*. 2015. doi:10.1002/art.39304.
- Sepriano A, Roman-Blas JA, Little RD, et al. DXA in the assessment of subchondral bone mineral density in knee osteoarthritis—a semi-standardized protocol after systematic review. *Semin Arthritis Rheum*. 2015. doi:10.1016/j.
- Lories RJ, Luyten FP. The bone-cartilage unit in osteoarthritis. *Nat Rev Rheumatol*. 2011;7(1):43–9.
- Zhen GH, Wen CY, Jia XF, Cao X. Inhibition of TGF- β signaling in mesenchymal stem cells of subchondral bone attenuates osteoarthritis. *Nat Med*. 2013;19(6):704–12.
- Patti GJ, Yanes O, Siuzdak G. Innovation: metabolomics: the pogue of the omics trilogy. *Nature reviews. Mol Cell Biol*. 2012;13(4):263–9.
- Zhang A, Sun H, Wang H. Serum metabolomics as a novel diagnostic approach for disease: a systematic review. *Anal Bioanal Chem*. 2012;404(4):1239–45.
- Kang J, Zhu L, Lu J, Zhang X. Application of metabolomics in autoimmune diseases: insight into biomarkers and pathology. *J Neuroimmunol*. 2015;279:25–32.
- Drexler DM, Reily MD, Shipkova PA. Advances in mass spectrometry applied to pharmaceutical metabolomics. *Anal Bioanal Chem*. 2011;399:2645–53.
- Puchades CL, Pineda LA. Metabolomics in pharmaceutical research and development. *Curr Opin Biotechnol*. 2015;35:73–7.
- Issaq HJ, Van QN, Waybright TJ, Muschik GM, Veenstra TD. Analytical and statistical approaches to metabolomics research. *J Sep Sci*. 2009;32(13):2183–99.
- Schuhmacher R, Krška R, Weckwerth W, Goodacre R. Metabolomics and metabolite profiling. *Anal Bioanal Chem*. 2013;405:5003–50004.
- Nordstrom A, O'Maille G, Qin C, Siuzdak G. Nonlinear data alignment for UPLC-MS and HPLC-MS based metabolomics: quantitative analysis of endogenous and exogenous metabolites in human serum. *Anal Chem*. 2006;78(10):3289–95.
- Grauso L, Mariggio S, Corda D, Fontana A, Cutignano A. An improved UPLC-MS/MS platform for quantitative analysis of glycerophosphoinositol in mammalian cells. *PLoS One*. 2015;10(4), e0123198.
- Adams SB, Setton LA, Nettles DL. The role of metabolomics in osteoarthritis research. *J An Acad Orthop Surg*. 2013;21(1):63–4.
- Li X, Yang SY, Qiu YP, et al. Urinary metabolomics as a potentially novel diagnostic and stratification tool for knee osteoarthritis. *Metabolomics*. 2010;6:109–18.
- Zhai GJ, Wang-Sattler R, Hart DJ, et al. Serum branched-chain amino acid to histidine ratio: a novel metabolomic biomarker of knee osteoarthritis. *Ann Rheum Dis*. 2010;69:1227–31.
- Damyantovich AZ, Staples JR, Chan AD, Marshall KW. Comparative study of normal and osteoarthritic canine synovial fluid using 500 MHz 1H magnetic resonance spectroscopy. *J Orthop Res*. 1999;17(2):223–31.
- Adams Jr SB, Setton LA, Kensicki E, Bolognesi MP, Toth AP, Nettles DL. Global metabolic profiling of human osteoarthritic synovium. *Osteoarthr Cartil*. 2012;20(1):64–7.
- Mickiewicz B, Kelly JJ, Ludwig TE, et al. Metabolic analysis of knee synovial fluid as a potential diagnostic approach for osteoarthritis. *J Orthop Res*. 2015. doi:10.1002/jor.22949.
- Altman R, Asch E, Bloch D, Bole G, Borenstein D. Development of criteria for the classification and reporting of osteoarthritis. Classification of osteoarthritis of the knee. Diagnostic and Therapeutic Criteria Committee of the American Rheumatism Association. *Arthritis Rheum*. 1986;29(8):1039–49.
- Kellgren JH, Lawrence JS. Radiological assessment of osteoarthrosis. *Ann Rheum Dis*. 1957;16(4):494–502.
- Want EJ, Masson P, Michopoulos F, Wilson ID. Global metabolic profiling of animal and human tissues via UPLC-MS. *Nat Protoc*. 2013;8(1):17–32.
- Sangster T, Major H, Plumb R, Wilson AJ, Wilson ID. A pragmatic and readily implemented quality control strategy for HPLC-MS and GC-MS-based metabolomic analysis. *Analyst (Cambridge, U K)*. 2006;131(10):1075–8.
- Solberg R, Escobar J, Arduini A, et al. Metabolomic analysis of the effect of postnatal hypoxia on the retina in a newly born piglet model. *PLoS One*. 2013;8(6), e66540.
- Bijlsma S, Bobeldijk I, Verheij ER, et al. Large-scale human metabolomics studies: a strategy for data (pre-) processing and validation. *Anal Chem*. 2006;78(2):567–74.
- Max B, Mattias R. OPLS discriminant analysis: combining the strengths of PLS-DA and SIMCA classification. *J Chemometrics*. 2006;20:341–51.
- Xia JG, David S. MetPA: a web-based metabolomics tool for pathway analysis and visualization. *Bioinformatics*. 2010;26(18):2342–4.
- Gika HG, Theodoridis GA, Wilson ID. Liquid chromatography and ultra-performance liquid chromatography–mass spectrometry fingerprinting of human urine: sample stability under different handling and storage conditions for metabolomics studies. *J Chromatogr A*. 2008;1189(1–2):314–22.
- Bylesjo M, Eriksson D, Trygg J. Orthogonal projections to latent structures as a strategy for microarray data normalization. *BMC Bioinformatics*. 2007;8:207.
- Lajeunesse D, Reboul P. Subchondral bone in osteoarthritis: a biologic link with articular cartilage leading to abnormal remodeling. *Curr Opin Rheumatol*. 2003;15(5):628–33.
- Sharif M, George E, Dieppe PA. Correlation between synovial fluid markers of cartilage and bone turnover and scintigraphic scan abnormalities in osteoarthritis of the knee. *Arthritis Rheum*. 1995;38(1):78–81.
- Lamers RJ, DeGroot J, Spies-Faber EJ, et al. Identification of disease- and nutrient-related metabolic fingerprints in osteoarthritic Guinea pigs. *J Nutr*. 2003;133(6):1776–80.
- Maher AD, Coles C, White J, et al. 1H NMR spectroscopy of serum reveals unique metabolic fingerprints associated with subtypes of surgically induced osteoarthritis in sheep. *J Proteome Res*. 2012;11(8):4261–8.
- Mickiewicz B, Heard BJ, Chau JK. Metabolic profiling of synovial fluid in a unilateral ovine model of anterior cruciate ligament reconstruction of the knee suggests biomarkers for early osteoarthritis. *J Orthop Res*. 2014;33(1):71–7.
- Okun JG, Kölker S, Schulze A, et al. A method for quantitative acylcarnitine profiling in human skin fibroblasts using unlabelled palmitic acid: diagnosis of fatty acid oxidation disorders and

- differentiation between biochemical phenotypes of MCAD deficiency. *Biochim Biophys Acta*. 2002;1584(2-3):91–8.
42. Seito N, Yamashita T, Tsukuda Y, et al. Interruption of glycerophospholipids synthesis enhances osteoarthritis development in mice. *Arthritis Rheum*. 2012;64(8):2579–88.
 43. Fukumoto S, Iwamoto T, Sakai E, et al. Current topics in pharmacological research on bone metabolism: osteoclast differentiation regulated by glycosphingolipids. *J Pharmacol Sci*. 2006;100(3):195–200.
 44. Ersek A, Xu K, Antonopoulos A, et al. Glycosphingolipid synthesis inhibition limits osteoclast activation and myeloma bone disease. *J Clin Invest*. 2015;125(6):2279–92.
 45. Mansell JP, Collins C, Bailey AJ. Bone, not cartilage, should be the major focus in osteoarthritis. *Nat Clin Pract Rheumatol*. 2007;3(6):306–7.
 46. Kosinska MK, Liebisch G, Lochnit G, et al. Sphingolipids in human synovial fluid—a lipidomic study. *PLoS One*. 2014;9(3), e91769.
 47. Joql G, Tong L. Crystal structure of carnitine acetyltransferase and implications for the catalytic mechanism and fatty acid transport. *Cell*. 2003;112(1):113–22.
 48. Nada MA, Rhead WJ, Sprecher H, Schulz H, Roe CR. Evidence for intermediate channeling in mitochondrial β -oxidation. *J Biol Chem*. 1995;270(2):530–5.
 49. Frey JL, Li Z, Ellis JM, et al. Wnt-lrp5 signaling regulates fatty acid metabolism in the osteoblast. *Mol Cell Biol*. 2015;35(11):1979–91.
 50. Colucci S, Mori G, Vaira S, et al. L-Carnitine and isovaleryl L-carnitine fumarate positively affect human osteoblast proliferation and differentiation in vitro. *Calcif Tissue Int*. 2005;76(6):458–65.
 51. Ge P, Cui Y, Liu F, Luan J, Zhou X, Han J. L-carnitine affects osteoblast differentiation in NIH3T3 fibroblasts by the IGF-1/PI3K/Akt signalling pathway. *Biosci Trends*. 2015;9(1):42–8.
 52. Orsal E, Halici Z, Bayir Y, et al. The role of carnitine on ovariectomy and inflammation-induced osteoporosis in rats. *Exp Biol Med (Maywood)*. 2013;238(12):1406–12.
 53. Abd-Allah AR, Al-Majed AA, Al-Yahya AA, Fouda SI, Al-Shabana OA. L-Carnitine halts apoptosis and myelosuppression induced by carboplatin in rat bone marrow cell cultures (BMC). *Arch Toxicol*. 2005;79(7):406–13.
 54. Xie H, Tang SY, Liu H, et al. L-Carnitine protects against apoptosis of murine MC3T3-E1 osteoblastic cells. *Amino Acids*. 2008;35(2):419–23.
 55. Patano N, Mancini L, Settanni MP, et al. L-Carnitine fumarate and isovaleryl-L-carnitine fumarate accelerate the recovery of bone volume/total volume ratio after experimentally induced osteoporosis in pregnant mice. *Calcif Tissue Int*. 2008;82(3):221–8.
 56. Aydin A, Halici Z, Albayrak A, et al. Treatment with carnitine enhances bone fracture healing under osteoporotic and/or inflammatory conditions. *Basic Clin Pharmacol Toxicol*. 2015;117(3):173–9.
 57. De Luca A, Pierno S, Camerino DC. Taurine: the appeal of a safe amino acid for skeletal muscle disorders. *J Transl Med*. 2015;13:243.
 58. Lubec B, Ya-hua Z, Perti S, Pentti T, Kitzmuller E, Lubec G. Distribution and disappearance of the radio labeled carbon derived from L-arginine and taurine in the mouse. *Life Sci*. 1997;60(26):2373–81.
 59. Zhou C, Zhang X, Xu L, Wu T, Cui L, Xu D. Taurine promotes human mesenchymal stem cells to differentiate into osteoblast through the ERK pathway. *Amino Acids*. 2014;46(7):1673–80.
 60. Park S, Kim H, Kim SJ. Stimulation of ERK2 by taurine with enhanced alkaline phosphatase activity and collagen synthesis in osteoblast-like UMR-106 cells. *Biochem Pharmacol*. 2001;62(6):1107–11.
 61. Yuan LQ, Xie H, Luo XH, et al. Taurine transporter is expressed in osteoblasts. *Amino Acids*. 2006;31(2):157–63.
 62. Chen SY, Yu HT, Kao JP, et al. An NMR metabolomic study on the effect of alendronate in ovariectomized mice. *PLoS One*. 2014;9(9), e106559.
 63. Yuan LQ, Liu W, Cui RR, et al. Taurine inhibits osteoclastogenesis through the taurine transporter. *Amino Acids*. 2010;39(1):89–99.
 64. Choi MJ, Chang KJ. Effect of dietary taurine and arginine supplementation on bone mineral density in growing female rats. *Adv Exp Med Biol*. 2013;776:335–45.
 65. Hügle T, Kovacs H, Heijnen IA, et al. Synovial fluid metabolomics in different forms of arthritis assessed by nuclear magnetic resonance spectroscopy. *Clin Exp Rheumatol*. 2012;30(2):240–5.
 66. Quesnele JJ, Laframboise MA, Wong JJ, Kim P, Wells GD. The effects of beta-alanine supplementation on performance: a systematic review of the literature. *Int J Sport Nutr Exerc Metab*. 2014;24(1):14–27.